

# Band offsets at amorphous-crystalline oxide interfaces: $\text{Al}_2\text{O}_3$ – $\text{SrTiO}_3$ as a model system

Dana Cohen-Azarzar, Maria Baskin, Lior Kornblum<sup>a)</sup>

The Andrew & Erna Faculty of Electrical Engineering, Technion – Israel Institute of Technology, Haifa 32000 – Israel

2D electron gases (2DEGs) formed at oxide interfaces provide a rich testbed for fundamental physics and device applications. While the discussion of the physical origins of this phenomena continues, the recent discovery of oxide 2DEGs at non-epitaxial interfaces between amorphous and crystalline oxides provides useful insight onto the debate. Using amorphous oxides further offers a low cost route towards realizing 2DEGs for device applications. In this work, the band offsets of a simple model system of amorphous-crystalline oxide interface are investigated. The model system consists of amorphous  $\text{Al}_2\text{O}_3$  grown on single-crystalline  $\text{SrTiO}_3$ . X-ray photoelectron spectroscopy is employed to study the chemical states, band gap and band offsets at the interface. The density of ionic defects near the interface is found to be below the detection limit, and the interface is found to be insulating. Analysis of the relative band structure yields significant interfacial barriers, exceeding 1 eV for holes and 2.3 eV for electrons. The barrier for holes is considerably larger than what is known for related materials systems, outlining the promise of using amorphous  $\text{Al}_2\text{O}_3$  as an effective and simple insulator, for future oxide-based field effect devices.

---

<sup>a)</sup> Author to whom correspondence should be addressed. Electronic mail: liork@technion.ac.il

The discovery of electron 2D electron gas (2DEG) at the epitaxial interface between two insulating oxides<sup>1</sup> has quickly led to the discovery of rich and unexpected physics.<sup>2-4</sup> These findings have sparked tremendous interest in multiple communities, ranging from fundamental physics, to materials science and to the engineering of various electronic and optoelectronic devices.<sup>5-10</sup>

The underlying physics of the 2DEG formation has been narrowed down to two leading mechanisms: a polarization mechanism and an ionic defects mechanism. The polarization mechanism, or the *polar catastrophe*, argues that polar discontinuity at the interface (along the [001] direction), typically between a non-polar SrTiO<sub>3</sub> substrate and a polar epitaxial overlayer such as LaAlO<sub>3</sub>, results in a diverging potential across the latter. The diverging potential is mitigated by an electronic reconstruction that often occurs above a critical thickness. In this case, ½ an electron per unit cell is transferred from the top surface to the interface, where it occupies Ti d-orbitals that form delocalized states.<sup>11,12</sup> Alternatively, the ionic mechanism highlights the role of defects, typically formed during the epitaxial growth of the overlayer<sup>13</sup> (e.g. LaAlO<sub>3</sub>). Some possible defects can act as dopants near the surface of SrTiO<sub>3</sub>. The most studied suspect in this context is the oxygen vacancy, a well-known electron donor in SrTiO<sub>3</sub>. Oxygen vacancies were shown to form readily at typical growth conditions of LaAlO<sub>3</sub>, resulting in interface conduction.<sup>14-17</sup> Additional ionic suspects for the formation of 2DEGs are ions such as La, that can diffuse into SrTiO<sub>3</sub> during epitaxial growth, where they function as dopants,<sup>18-21</sup> as well as other electronically-active defects.<sup>22,23</sup> Ample experimental evidence supporting both mechanisms suggests that there is no single culprit behind the 2DEG phenomena.

To make things more interesting, it was later discovered<sup>24,25</sup> that 2DEGs can be formed at non-epitaxial interfaces, between a single-crystal substrate and amorphous oxides, with chemical evidence correlating the presence of oxygen vacancies in proximity to the SrTiO<sub>3</sub> with the interface carrier density. This observation demonstrates that similar 2DEGs can be obtained in a material system where polar catastrophe is not possible, due to the absence of long-range order. These observations do not categorically rule out polar catastrophe, rather they underscore the complexity of the problem and highlight the importance of the surface chemistry, the oxidation states and interface electrostatics. A key aspect in this picture is the relative offsets between the bands at the interface. This aspect has been thoroughly studied in polar/non-polar epitaxial interfaces such as GdTlO<sub>3</sub>/SrTiO<sub>3</sub>,<sup>26,27</sup>  $\gamma$ -Al<sub>2</sub>O<sub>3</sub>/SrTiO<sub>3</sub>,<sup>28,29</sup> NdTiO<sub>3</sub>/SrTiO<sub>3</sub>,<sup>30,31</sup> LaNiO<sub>3</sub>/SrTiO<sub>3</sub>,<sup>26</sup> SmTiO<sub>3</sub>/SrTiO<sub>3</sub>,<sup>27</sup> LaCrO<sub>3</sub>/SrTiO<sub>3</sub>,<sup>32</sup> and LaAlO<sub>3</sub>/SrTiO<sub>3</sub>,<sup>21,33-36</sup> providing valuable physical insight, such as the existence<sup>32</sup> or absence<sup>28,37</sup> of polarization-induced internal fields, substrate band bending<sup>28</sup> and effects of ion intermixing<sup>21</sup> and oxygen vacancies.<sup>35</sup>

Despite this wealth of data on crystalline epitaxial interfaces, to our knowledge the band offsets at amorphous/crystalline oxide interfaces has not been addressed. These interfaces allow a clear look at the electronic structure at the interface in the absence of polar fields. Motivated by this knowledge gap, we study the surface chemistry, electronic structure and relative band offsets at a model amorphous-crystalline interface between Al<sub>2</sub>O<sub>3</sub> and SrTiO<sub>3</sub> (STO).

TiO<sub>2</sub> termination was performed on undoped, 0.5 and 0.7% (wt) Nb-doped STO substrates (Crystal GmbH, Shinkosha Corp. and MTI Corp.) following the ‘extended Arkansas’ method.<sup>38</sup> The process started with solvent sonication cleaning, followed by a 3:1 HCl-HNO<sub>3</sub> treatment, and a two-step anneal, starting with 1,000°C for 1 hr in air and completed with 650°C for 30 min in flowing O<sub>2</sub>. Amorphous Al<sub>2</sub>O<sub>3</sub> layers were grown by atomic layer deposition (ALD, Ultratech/Cambridge Nanotech Fiji G2) using trimethyl-aluminum (TMA) and water as precursors at a substrate temperature of 250°C. 4 and 10 nm thick layers were grown: the thin layer puts both the Al<sub>2</sub>O<sub>3</sub> and the substrate within the probing depth of x-ray photoelectron spectroscopy (XPS), whereas only Al<sub>2</sub>O<sub>3</sub> is probed in the thick layer. The thicknesses of the layers were found to be in close agreement with the nominal values (within 3%) with x-ray reflectivity. The layers are referred to as Thin Al<sub>2</sub>O<sub>3</sub> and Thick Al<sub>2</sub>O<sub>3</sub> henceforth.

An atomic force microscopy (AFM, Asylum MFP-3D Infinity) image was acquired in tapping mode from the top of the thin Al<sub>2</sub>O<sub>3</sub> (Fig. 1a). The observation of long range atomically-flat terraces with atomic height steps indicates that the roughness of the thin Al<sub>2</sub>O<sub>3</sub> layer is well below the ~0.4 nm step height. XPS (Thermo VG Scientific Sigma Probe) was acquired using Al K $\alpha$  source (1486.6 eV) and a pass energy of 30 eV. Data was fit with the CasaXPS software using a Shirley background, a 30% Lorentzian-Gaussian ratio. The Ti 2p XPS spectrum of the clean STO surface (Fig. 1b) shows a well-behaved +4 state<sup>39</sup> and no +3 oxidation states are observable at lower binding energies,<sup>40</sup> further validating the surface preparation procedure.

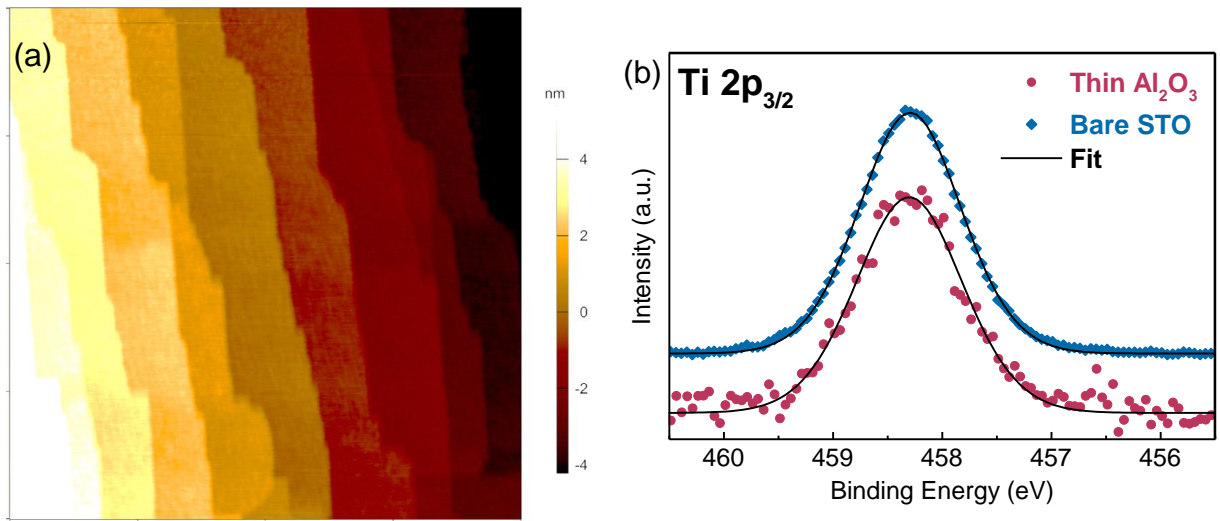


**FIG. 1.** (a) Tapping mode AFM image of the surface of a  $2 \times 2 \mu\text{m}$  region of the surface of a thin  $\text{Al}_2\text{O}_3$  layer (4 nm) on undoped STO. (b) Ti 2p XPS spectrum of the clean surface superimposed on the Ti 2p spectrum, obtained from underneath the thin  $\text{Al}_2\text{O}_3$  (4 nm) layer.

The thick  $\text{Al}_2\text{O}_3$  layer is used for studying the properties of  $\text{Al}_2\text{O}_3$  without interference from the substrate. The Al 2p spectrum (Fig. 2a) shows well-behaved features that are fit with one doublet having a 0.4eV separation,<sup>46</sup> showing a single oxidation state consistent with  $\text{Al}_2\text{O}_3$ .<sup>41</sup> Analysis of the O 1s region reveals a major component that is ascribed to  $\text{Al}_2\text{O}_3$  ('Peak 1'), and two minor moieties ('Peaks 2,3'), attributed to surface contamination (Fig. 2b). The uncertainty in the position of the small contamination peaks has negligible effect on the position of the major O 1s component of the  $\text{Al}_2\text{O}_3$  film.<sup>42</sup> The distance of the onset of the energy loss tail<sup>43,44</sup> from the major O 1s ( $\text{Al}_2\text{O}_3$ ) peak yields a bandgap of  $6.6 \pm 0.2$  eV (denoted by a horizontal arrow in the inset of Fig. 2b). This value is in agreement with previous reports for amorphous  $\text{Al}_2\text{O}_3$ .<sup>44-46</sup>

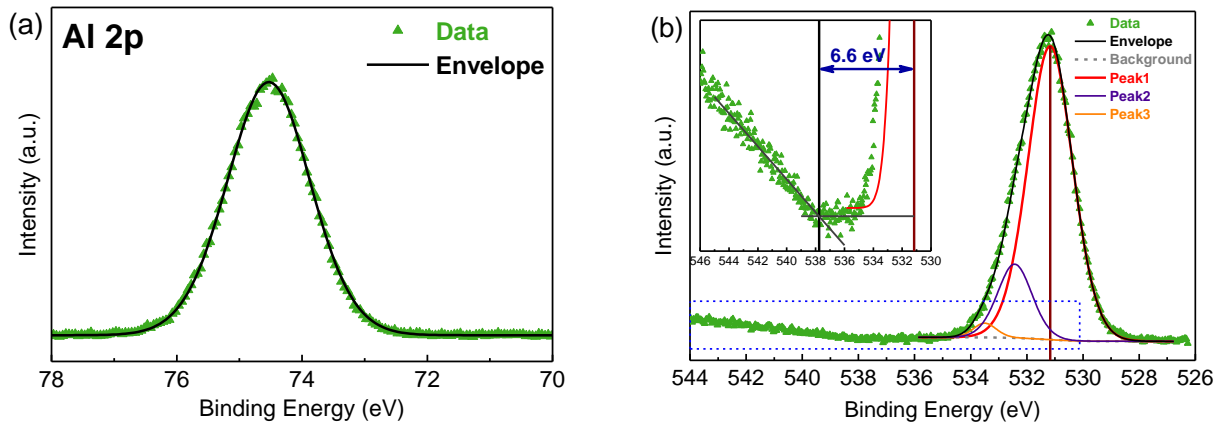


**FIG. 2.**  $\text{Al}_2\text{O}_3$  properties. XPS analysis of a Thick  $\text{Al}_2\text{O}_3$  (10 nm). (a) Al 2p spectrum, (b) O 1s spectrum. The inset shows a magnified region of the energy loss tail region, taken from the dashed blue rectangle. The vertical lines represent the centroid of the major O 1s peak (red) and the intersection of the linear fit of the loss tail with the background<sup>44</sup> (black). The distance between the lines (black horizontal arrow) denotes the band gap of  $\text{Al}_2\text{O}_3$ .

Al contacts<sup>47</sup> were deposited on the corners of the wafers (e-beam deposition) after scratching them to contact the interface.<sup>48</sup> The resistance of the films was beyond the measurement limit ( $>5\text{M}\Omega$ ), indicating that the sheet carrier density is lower than  $10^{11} \text{ cm}^{-2}$ . This observation is in agreement with the absence of  $\text{Ti}^{+3}$  signal in the Ti 2p spectrum acquired at the interface with  $\text{Al}_2\text{O}_3$  (thin  $\text{Al}_2\text{O}_3$ ), Fig. 1b. Similar observations were also made by Susaki et al. using hard x-ray photoemission spectroscopy (HAXPS) at polar  $\text{LaAlO}_3$ -STO interfaces.<sup>36</sup> Considering the noisy background we conclude that  $\text{Ti}^{+3}$  could account for as much as 3% of the signal. The insulating character of these  $\text{Al}_2\text{O}_3$ -STO interfaces is ascribed to the low temperature ALD process, which inhibits the surface reduction of STO,<sup>25</sup> in contrast to some higher temperature routes where reduction is more pronounced.<sup>29</sup> The ability to obtain an insulating interface, without significant oxygen vacancies, is interesting for some

applications; insulator-STO interfaces with low defect densities are sought for various devices, and complex routes are utilized to create such interfaces.<sup>49,50</sup>

Alignment of the energy scales of the different samples is done as follows: First, the energy scales of both the thick and thin Al<sub>2</sub>O<sub>3</sub> layers are aligned so that the Al 2p<sub>3/2</sub> peak of each is positioned at 74.4 eV.<sup>46</sup> The energy scale of the bare STO substrate is then aligned as such that the Ti 2p<sub>3/2</sub> peak is at the same energy the same feature from underneath the thin Al<sub>2</sub>O<sub>3</sub> layer (Fig. 3a). This systematic alignment of the energy scale allows the direct comparison of the valence band edges of Al<sub>2</sub>O<sub>3</sub> and undoped STO, yielding the valence band offset of 1.0±0.2 eV at the interface.<sup>51–53</sup> Kormondy and coworkers reported an offset of 0.9 eV for crystalline  $\gamma$ -Al<sub>2</sub>O<sub>3</sub>, epitaxially grown on STO,<sup>29</sup> and while  $\gamma$ -Al<sub>2</sub>O<sub>3</sub> has a different band structure compared to the amorphous phase, we note the similarity of these values.

This analysis was further extended to 0.5 and 0.7% (wt) Nb-doped STO substrates, yielding valence band offsets of 1.1±0.2 and 1.15±0.2 eV, respectively (Fig. 3b, 3c). These valence band offsets are considerably larger than reported values of 0.0-0.6 eV for the LaAlO<sub>3</sub>-STO interface.<sup>33,35,36</sup> The larger valence band offset (and band gap) measured here imply that Al<sub>2</sub>O<sub>3</sub> may be a better insulator than the more common LaAlO<sub>3</sub> and  $\gamma$ -Al<sub>2</sub>O<sub>3</sub> for field effect devices.<sup>10</sup> This observation highlights the promise of ALD-grown Al<sub>2</sub>O<sub>3</sub> to provide a simple route towards field effect devices based on oxide 2DEGs.

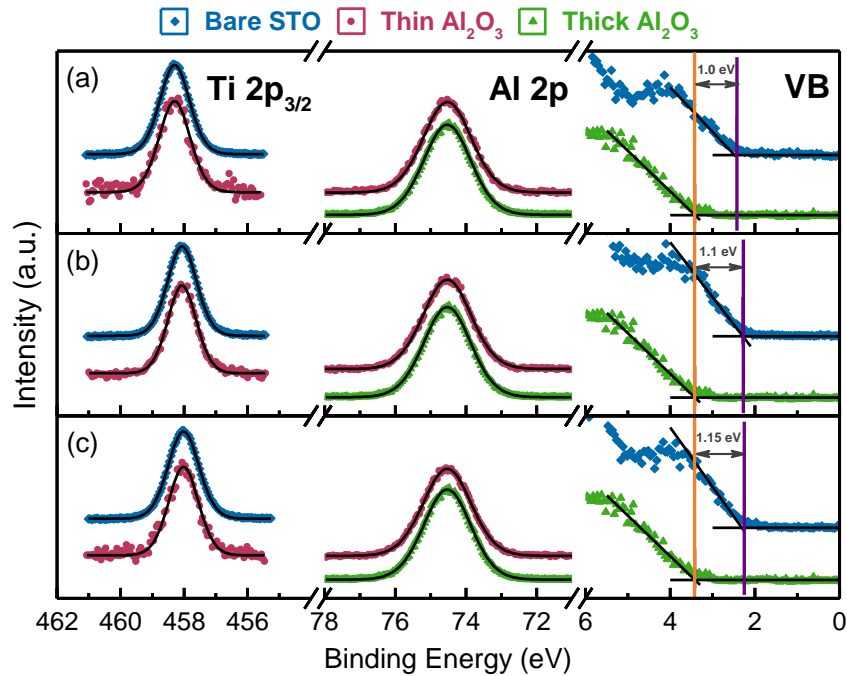


**FIG. 3.** Band alignment analysis of the Al<sub>2</sub>O<sub>3</sub>-STO. The Al 2p, Ti 2p and valence band (VB) spectra of a Bare STO substrate, Thin Al<sub>2</sub>O<sub>3</sub> (4 nm) and Thick Al<sub>2</sub>O<sub>3</sub> (10 nm) are shown for (a) undoped, (b) 0.5% (wt) and (c) 0.7% (wt) Nb-doped STO substrates. The Thick Al<sub>2</sub>O<sub>3</sub> data (green triangles) is duplicated from panel a to panels b and c for clarity.

Combining the measured valence band offsets with the bandgap of Al<sub>2</sub>O<sub>3</sub> of 6.6 eV (Fig. 2b) and the bandgap of STO, 3.2 eV (which does not change over the doping range used here<sup>53</sup>), the conduction band offsets are determined as 2.4, 2.3 and 2.25±0.3 eV for undoped, 0.5% and 0.7% (wt) Nb, respectively (Fig. 4). An uncertainty range of ±0.2 eV is estimated from the determination of the valence band edge and the band gap (accumulating to ±0.3 eV when both are factored in), whereas the peaks are fit with uncertainties <0.05 eV. We therefore conclude that substrate doping has an effect smaller than the uncertainty of 0.2 eV on the valence band offsets at Al<sub>2</sub>O<sub>3</sub>-STO interfaces.

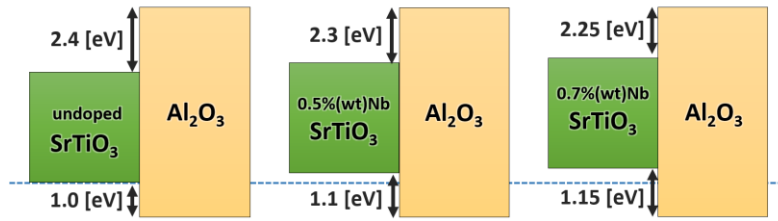


**FIG. 4.** Schematic relative band structure at the  $\text{Al}_2\text{O}_3$ -STO interface. The dashed line serves as a reference for the position of the valence band of undoped STO. The relative distances are not to scale.

In summary, non-polar amorphous  $\text{Al}_2\text{O}_3$ -STO oxide interfaces prepared by a low temperature process were studied. The interface was found to be insulating, with a low density of ionic defects – below the measurement limit of XPS. The large band gap of amorphous  $\text{Al}_2\text{O}_3$  results in offsets larger than what was reported for related material systems, constituting significant interface barriers for both holes and electrons. The effect of STO doping on the band offsets is smaller than the 0.2 eV analysis uncertainty, in the range of 0-0.7% (wt) Nb. These results highlight the potential of  $\text{Al}_2\text{O}_3$  as an insulator for STO-based oxide electronics.

## ACKNOWLEDGMENTS

The authors thank the Technion's Russell Berrie Nanotechnology Institute (RBNI) for partial support of this work. Sample fabrication was done with the support of the Technion's micro-nano fabrication unit (MNFU). The authors thank Dr. Kamira Weinfeld for her assistance with XPS acquisition, and Dr. Boris Meyler, Valentina Korchnoy and Tatiana Beker for their valuable assistance with fabrication and processing of the samples.

## REFERENCES

- <sup>1</sup> A. Ohtomo and H.Y. Hwang, *Nature* **427**, 423 (2004).
- <sup>2</sup> J.A. Bert, B. Kalisky, C. Bell, M. Kim, Y. Hikita, H.Y. Hwang, and K.A. Moler, *Nat Phys* **7**, 767 (2011).
- <sup>3</sup> D.A. Dikin, M. Mehta, C.W. Bark, C.M. Folkman, C.B. Eom, and V. Chandrasekhar, *Phys. Rev. Lett.* **107**, 56802 (2011).
- <sup>4</sup> L. Li, C. Richter, J. Mannhart, and R.C. Ashoori, *Nat Phys* **7**, 762 (2011).
- <sup>5</sup> S. Stemmer, P. Moetakef, T. Cain, C. Jackson, D. Ouellette, J.R. Williams, D. Goldhaber-Gordon, L. Balents, and S.J. Allen, *IEEE Proc. SPIE* **8626**, 86260F (2013).
- <sup>6</sup> G. Cheng, P.F. Siles, F. Bi, C. Cen, D.F. Bogorin, C.W. Bark, C.M. Folkman, J.-W. Park, C.-B. Eom, G. Medeiros-Ribeiro, and J. Levy, *Nat Nano* **6**, 343 (2011).
- <sup>7</sup> N. Pryds and V. Esposito, *J. Electroceramics* **38**, 1 (2016).
- <sup>8</sup> S. Gariglio, M. Gabay, and J.-M. Triscone, *APL Mater.* **4**, 60701 (2016).
- <sup>9</sup> J. Mannhart, D.H.A. Blank, H.Y. Hwang, A.J. Millis, and J.-M. Triscone, *MRS Bull.* **33**, 1027 (2011).
- <sup>10</sup> R. Jany, C. Richter, C. Woltmann, G. Pfanzelt, B. Förg, M. Rommel, T. Reindl, U. Waizmann, J. Weis, J.A. Mundy, D.A. Muller, H. Boschker, and J. Mannhart, *Adv. Mater. Interfaces* **1**, 1300031 (2014).
- <sup>11</sup> N. Pavlenko, T. Kopp, E.Y. Tsymbal, J. Mannhart, and G.A. Sawatzky, *Phys. Rev. B* **86**, 64431 (2012).
- <sup>12</sup> A. Janotti, L. Bjaalie, L. Gordon, and C.G. Van de Walle, *Phys. Rev. B* **86**, 241108 (2012).
- <sup>13</sup> A.B. Posadas, K.J. Kormondy, W. Guo, P. Ponath, J. Geler-Kremer, T. Hadamek, and A.A. Demkov, *J. Appl. Phys.* **121**, 105302 (2017).

- <sup>14</sup> G. Herranz, M. Basletić, M. Bibes, C. Carrétéro, E. Tafra, E. Jacquet, K. Bouzehouane, C. Deranlot, A. Hamzić, J.-M. Broto, A. Barthélémy, and A. Fert, *Phys. Rev. Lett.* **98**, 216803 (2007).
- <sup>15</sup> Z.Q. Liu, C.J. Li, W.M. Lü, X.H. Huang, Z. Huang, S.W. Zeng, X.P. Qiu, L.S. Huang, A. Annadi, J.S. Chen, J.M.D. Coey, T. Venkatesan, and Ariando, *Phys. Rev. X* **3**, 21010 (2013).
- <sup>16</sup> F. Gunkel, R. Waser, A.H.H. Ramadan, R.A. De Souza, S. Hoffmann-Eifert, and R. Dittmann, *Phys. Rev. B* **93**, 245431 (2016).
- <sup>17</sup> C. Xu, C. Bäumer, R.A. Heinen, S. Hoffmann-Eifert, F. Gunkel, and R. Dittmann, *Sci. Rep.* **6**, 22410 (2016).
- <sup>18</sup> S.A. Pauli, S.J. Leake, B. Delley, M. Björck, C.W. Schneider, C.M. Schlepütz, D. Martocchia, S. Paetel, J. Mannhart, and P.R. Willmott, *Phys. Rev. Lett.* **106**, 36101 (2011).
- <sup>19</sup> L. Qiao, T.C. Droubay, T. Varga, M.E. Bowden, V. Shutthanandan, Z. Zhu, T.C. Kaspar, and S.A. Chambers, *Phys. Rev. B* **83**, 85408 (2011).
- <sup>20</sup> E. Breckenfeld, N. Bronn, J. Karthik, A.R. Damodaran, S. Lee, N. Mason, and L.W. Martin, *Phys. Rev. Lett.* **110**, 196804 (2013).
- <sup>21</sup> C. Weiland, G.E. Sterbinsky, A.K. Rumaiz, C.S. Hellberg, J.C. Woicik, S. Zhu, and D.G. Schlom, *Phys. Rev. B* **91**, 165103 (2015).
- <sup>22</sup> L. Yu and A. Zunger, *Nat. Commun.* **5**, 5118 (2014).
- <sup>23</sup> F. Gunkel, C. Bell, H. Inoue, B. Kim, A.G. Swartz, T.A. Merz, Y. Hikita, S. Harashima, H.K. Sato, M. Minohara, S. Hoffmann-Eifert, R. Dittmann, and H.Y. Hwang, *Phys. Rev. X* **6**, 31035 (2016).
- <sup>24</sup> Y. Chen, N. Pryds, J.E. Kleibeuker, G. Koster, J. Sun, E. Stamate, B. Shen, G. Rijnders, and S. Linderorth, *Nano Lett.* **11**, 3774 (2011).
- <sup>25</sup> S.W. Lee, Y. Liu, J. Heo, and R.G. Gordon, *Nano Lett.* **12**, 4775 (2012).
- <sup>26</sup> G. Conti, A.M. Kaiser, A.X. Gray, S. Nemšák, G.K. Pálsson, J. Son, P. Moetakef, A. Janotti, L. Bjaalie, C.S. Conlon, D. Eiteneer, A.A. Greer, A. Keqi, A. Rattanachata, A.Y. Saw, A. Bostwick, W.C. Stolte, A. Gloskovskii, W. Drube, S. Ueda, M. Kobata, K. Kobayashi, C.G. de Walle, S. Stemmer, C.M. Schneider, and C.S. Fadley, *J. Appl. Phys.* **113**, 143704 (2013).
- <sup>27</sup> L. Bjaalie, A. Azcatl, S. McDonnell, C.R. Freeze, S. Stemmer, R.M. Wallace, and C.G. de Walle, *J. Vac. Sci. Technol. A* **34**, 61102 (2016).
- <sup>28</sup> P. Schütz, F. Pfaff, P. Scheiderer, Y.Z. Chen, N. Pryds, M. Gorgoi, M. Sing, and R. Claessen, *Phys. Rev. B* **91**, 165118 (2015).
- <sup>29</sup> K.J. Kormondy, A.B. Posadas, T.Q. Ngo, S. Lu, N. Goble, J. Jordan-Sweet, X.P.A. Gao, D.J. Smith, M.R. McCartney, J.G. Ekerdt, and A.A. Demkov, *J. Appl. Phys.* **117**, (2015).
- <sup>30</sup> P. Xu, T.C. Droubay, J.S. Jeong, K.A. Mkhoyan, P. V Sushko, S.A. Chambers, and B. Jalan, *Adv. Mater. Interfaces* **3**, 1500432 (2016).
- <sup>31</sup> P. Xu, Y. Ayino, C. Cheng, V.S. Pribiag, R.B. Comes, P. V Sushko, S.A. Chambers, and B. Jalan, *Phys. Rev. Lett.* **117**, 106803 (2016).
- <sup>32</sup> S.A. Chambers, L. Qiao, T.C. Droubay, T.C. Kaspar, B.W. Arey, and P. V Sushko, *Phys. Rev. Lett.* **107**, 206802 (2011).
- <sup>33</sup> S.A. Chambers, M.H. Engelhard, V. Shutthanandan, Z. Zhu, T.C. Droubay, L. Qiao, P. V Sushko, T. Feng, H.D. Lee, T. Gustafsson, E. Garfunkel, A.B. Shah, J.-M. Zuo, and Q.M. Ramasse, *Surf. Sci. Rep.* **65**, 317 (2010).
- <sup>34</sup> L. Qiao, T.C. Droubay, T.C. Kaspar, P. V Sushko, and S.A. Chambers, *Surf. Sci.* **605**, 1381 (2011).
- <sup>35</sup> G. Berner, A. Müller, F. Pfaff, J. Walde, C. Richter, J. Mannhart, S. Thiess, A. Gloskovskii, W. Drube, M. Sing, and R. Claessen, *Phys. Rev. B* **88**, 115111 (2013).
- <sup>36</sup> T. Susaki, S. Ueda, K. Matsuzaki, T. Kobayashi, Y. Toda, and H. Hosono, *Phys. Rev. B* **94**, 75311 (2016).
- <sup>37</sup> Y. Segal, J.H. Ngai, J.W. Reiner, F.J. Walker, and C.H. Ahn, *Phys. Rev. B* **80**, 241107 (2009).

- <sup>38</sup> J. Zhang, D. Doust, T. Merz, J. Chakhalian, M. Kareev, J. Liu, and L.J. Brillson, *Appl. Phys. Lett.* **94**, 92904 (2009).
- <sup>39</sup> R.T. Haasch, E. Breckenfeld, and L.W. Martin, *Surf. Sci. Spectra* **21**, 87 (2014).
- <sup>40</sup> M.S.J. Marshall, D.T. Newell, D.J. Payne, R.G. Egdell, and M.R. Castell, *Phys. Rev. B* **83**, 35410 (2011).
- <sup>41</sup> L. Kornblum, J.A. Rothschild, Y. Kauffmann, R. Brener, and M. Eizenberg, *Phys. Rev. B* **84**, 155317 (2011).
- <sup>42</sup> L. Kornblum, B. Meyler, J. Salzman, and M. Eizenberg, *J. Appl. Phys.* **113**, 74102 (2013).
- <sup>43</sup> S. Miyazaki, *J. Vac. Sci. Technol. B* **19**, 2212 (2001).
- <sup>44</sup> I. Geppert, E. Lipp, R. Brener, S. Hung, and M. Eizenberg, *J. Appl. Phys.* **107**, 53701 (2010).
- <sup>45</sup> M.L. Huang, Y.C. Chang, C.H. Chang, T.D. Lin, J. Kwo, T.B. Wu, and M. Hong, *Appl. Phys. Lett.* **89**, 12903 (2006).
- <sup>46</sup> E. Bersch, S. Rangan, R.A. Bartynski, E. Garfunkel, and E. Vescovo, *Phys. Rev. B* **78**, 85114 (2008).
- <sup>47</sup> L. Kornblum, E.N. Jin, O. Shoron, M. Boucherit, S. Rajan, C.H. Ahn, and F.J. Walker, *J. Appl. Phys.* **118**, 105301 (2015).
- <sup>48</sup> L. Kornblum, E.N. Jin, D.P. Kumah, A.T. Ernst, C.C. Broadbridge, C.H. Ahn, and F.J. Walker, *Appl. Phys. Lett.* **106**, 201602 (2015).
- <sup>49</sup> N. Kumar, A. Kitoh, and I.H. Inoue, *Sci. Rep.* **6**, 25789 (2016).
- <sup>50</sup> A. Schulman, A. Kitoh, P. Stoliar, and I.H. Inoue, *Appl. Phys. Lett.* **110**, 13502 (2017).
- <sup>51</sup> S.A. Chambers, Y. Liang, Z. Yu, R. Droopad, J. Ramdani, and K. Eisenbeiser, *Appl. Phys. Lett.* **77**, 1662 (2000).
- <sup>52</sup> L. Kornblum, M.D. Morales-Acosta, E.N. Jin, C.H. Ahn, and F.J. Walker, *Adv. Mater. Interfaces* **2**, 201500193 (2015).
- <sup>53</sup> K.J. May, D.P. Fenning, T. Ming, W.T. Hong, D. Lee, K.A. Stoerzinger, M.D. Biegalski, A.M. Kolpak, and Y. Shao-Horn, *J. Phys. Chem. Lett.* **6**, 977 (2015).